A plasma model combined with an improved two-temperature equation for ultrafast laser ablation of dielectrics

Lan Jiang[1,2,a)] and Hai-Lung Tsai[2]
[1]*Laser Micro-/Nano-Fabrication Laboratory, Department of Mechanical and Automation Engineering, 3rd School, Beijing Institute of Technology, Beijing 100081, People's Republic of China*
[2]*Laser-Based Manufacturing Laboratory, Department of Mechanical and Aerospace Engineering, Missouri University of Science and Technology Rolla (formerly University of Missouri-Rolla), Missouri 65409,USA*

(Received 28 June 2008; accepted 9 September 2008; published online 4 November 2008)

It remains a big challenge to theoretically predict the material removal mechanism in femtosecond laser ablation. To bypass this unresolved problem, many calculations of femtosecond laser ablation of nonmetals have been based on the free electron density distribution without the actual consideration of the phase change mechanism. However, this widely used key assumption needs further theoretical and experimental confirmation. By combining the plasma model and improved two-temperature model developed by the authors, this study focuses on investigating ablation threshold fluence, depth, and shape during femtosecond laser ablation of dielectrics through nonthermal processes (the Coulomb explosion and electrostatic ablation). The predicted ablation depths and shapes in fused silica, by using (1) the plasma model only and (2) the plasma model plus the two-temperature equation, are both in agreement with published experimental data. The widely used assumptions for threshold fluence, ablation depth, and shape in the plasma model based on free electron density are validated by the comparison study and experimental data. © *2008 American Institute of Physics*. [DOI: 10.1063/1.3006129]

I. INTRODUCTION

A femtosecond pulse laser can fully ionize almost any solid material with reduced recast, microcracks, and heat-affected zone. Hence, femtosecond lasers are promising for the micro/nanoscale fabrication of all types of materials[1–4] especially dielectrics.[1,2] Building up of free electrons is necessary in order to initialize laser ablation of dielectrics. Once the critical free electron density is created, the transparent material becomes opaque, and the absorbed energy is mainly deposited in a very thin layer within a short period of time, which leads to the ablation of the thin layer. Energy transport within the bulk material during the ablation process can be divided into two stages:[4–9] (1) the photon energy absorption, mainly through free electrons generation, heating, and electron excitation in a time scale from a few femtoseconds to a few picoseconds and (2) the redistribution of the absorbed energy to lattice leading to material removal in a time scale from a few picoseconds to a few nanoseconds.

Although many studies have been conducted, there remain some challenges in predicting femtosecond laser ablation, especially the dissipation of the absorbed energy into lattice and the corresponding material removal mechanisms.[10,11] The specific phase change mechanism depends on the fluence, pulse duration, wavelength, repetition rate, pulse number, and material properties.[10] The major phase change mechanisms include thermal processes (nonequilibrium thermal vaporization and melting) and nonthermal processes (the Coulomb explosion and electrostatic ablation). The four competing mechanisms may coexist or transit to each other,[10] which still cannot be theoretically determined.

To bypass the unresolved problems in material removal mechanisms, many calculations of femtosecond laser ablation shape of nonmetals have been based on free electron density distribution without the actual consideration of the phase change.[1,12–19] Comparing with material removals, the free electron generation and heating are much better understood.[1,12–16] Stuart and co-workers[12–14] developed theories for free electron generation based on the kinetic equation and experimental results for the ablation of dielectrics at 1053, 852, and 526 nm wavelengths and 100 fs–1 ns pulsewidths. Jiang and Tsai[1,15,16] further improved the methodology into a plasma model with quantum treatments to predict the ablation depth and crater shape.

The common-platform key assumptions of the works above[1,12–19] are all based on free electron density distribution without the actual consideration of the phase change, which needs further theoretical and experimental confirmations. By combining the plasma model[1,16] and improved two-temperature model[3] developed by the authors, this study focuses on femtosecond laser ablation of dielectrics through nonthermal processes (the Coulomb explosion and electrostatic ablation). The model simplified from the Fokker–Planck equation is employed to calculate the free electron generation through the impact ionization and photoionization processes. The quantum theories are used to calculate the free electron heating, free electron relaxation time, and the spatial and temporal dependent optical properties for the dense plasma generated by the femtosecond pulse. Because the dielectric material is first transformed into absorbing

a)Author to whom correspondence should be addressed. Tel.: +86-10-6891-4517. Electronic addresses: jianglan@bit.edu.cn and jianglan@mst.edu.

plasma with metallic properties by strong ionization before phase change occurs, the improved two-temperature model can be applied to describe the electron-phonon interaction in the impact area. The predicted ablation threshold fluence, depth, and shape of fused silica are in agreement with the published experimental data. The widely used assumptions for threshold fluence, ablation depth, and shape based on generated free electron density in dense plasma are validated by the comparison study.

II. THEORY

A. Assumptions

The main purpose of this study is to compare the predictions by using following two types of assumptions: (1) the assumptions based on free electron density in the plasma model[1,16] and (2) the assumptions based on lattice temperature in the plasma model combined with the two-temperature equation.[3]

1. Free electron density based assumptions

It is widely assumed that the ablation starts when the free electron density reaches the critical density.[1,12–19] Hence, threshold fluence can be considered as the minimal fluence that just creates the critical density.[1,12–19] Since the free electrons in the thin laser irradiation layer are excited up to tens of electron volts, the Coulomb explosion, electrostatic ablation, or nonequilibrium thermal ablation, instead of melting, dominate the phase change after the ionization process.[6,10,11,17] Thus, under a femtosecond pulse irradiation, hydrodynamic (liquid phase) motion of dielectrics is generally negligible. As a result, comparing with long pulses (>10 ps), melting and recast are greatly reduced and negligible, especially at fluences that are not much higher than the threshold fluence.

In the limit of negligible recast, ablation depth can be considered to be the maximum depth at which the maximum free electron density is equal to the critical density in a given processing window.[12–14] Similarly, the ablation crater shape corresponds to the ionized region at which the free electron density is greater than or equal to the critical density.

2. Lattice temperature based assumptions

In broad thermodynamic areas, most of the material removal assumptions are made according to the lattice/material temperature: the phase change happens if the lattice/material temperature increases above a certain characteristic point. For the femtosecond laser ablation of dielectrics at fluences slightly higher than the threshold fluence, the Coulomb explosion, electrostatic ablation, and/or nonequilibrium thermal ablation dominates and melting is insignificant. The material is removed if the temperature is higher than the vaporization temperature. On the other hand, in a temperature-based assumption, it is relatively easy to include the insignificant melting also. Hence, we assume that the phase change happens when the lattice temperature is higher than the melting temperature (softening point for glasses). Actually, the melt part of the dielectrics (although insignificant) can also later be removed by the pressure and strong electric field generated by the femtosecond pulse, since the impact area is strongly ionized. Hence, in this study, it is assumed that a part will be removed if its temperature is higher than the melting point that is 1988 K for fused silica glass.

B. Free electron generation: Ionization

The following expression derived from the Fokker–Planck equation is used to calculate the free electron generation,[12–14] in which the electron decay term is also considered[19]

$$\frac{\partial n_e(t,r,z)}{\partial t} = a_i I(t,r,z) n_e(t,r,z) + \delta_N [I(t,r,z)]^N, \tag{1}$$

where t is the time, r is the distance to the Gaussian beam axis, z is the depth from the surface of the bulk material, τ is the decay time constant, $n_e(t,r,z)$ is the free electron density, a_i is the impact ionization constant, $I(t,r,z)$ is the laser intensity inside the bulk material, and δ_N is the cross-section of N-photon absorption. Based on experimental measurements of the threshold fluences,[2] at the wavelength of 780 nm for fused silica, $a_i = 4 \pm 0.6$ cm^2/J, $\delta_6 = 6 \times 10^{8\pm0.9}$ cm^{-3} ps^{-1}(cm^2/T W)^6.

C. Laser-plasma interaction: Optical properties

The original laser beam before it interacts with the material is assumed to be a Gaussian distribution in time and space. It is assumed that the laser focus point is at the material surface, $z=0$. Considering time and space dependent optical properties, the laser intensities inside the bulk materials are expressed as[16]

$$I(t,r,z) = \frac{2F}{\sqrt{\pi/\ln 2}\, t_p}[1 - R(t,r)] \times \exp\left[-\frac{r^2}{r_0^2} - (4 \ln 2) \times \left(\frac{t}{t_p}\right)^2 - \int_0^z \alpha(t,r,z)dz \right], \tag{2}$$

where F is the laser fluence, t_p is the pulse duration, $R(t,r)$ is the reflectivity, r_0 is the radius of the laser beam that is defined as the distance from the center at which the intensity drops to $1/e^2$ of the maximum intensity, and $\alpha(t,r,z)$ is the absorption coefficient. The optical properties of the highly ionized dielectrics under a femtosecond pulse can be well determined by plasma properties.[2] In this study, the Drude model for the plasma in the metals and doped semiconductors is used to determine the optical properties of the ionized dielectrics. The spatial and temporal dependent dielectric function of the plasma is expressed as[20]

$$\epsilon(t,r,z) = 1 + \left(\frac{n_e(t,r,z)e^2}{m_e \epsilon_0}\right)\left(\frac{-\tau_e^2(t,r,z) + i\tau_e(t,r,z)/\omega}{1 + \omega^2 \tau_e^2(t,r,z)}\right), \tag{3}$$

where e is the electron charge, m_e is the mass of electron, ϵ_0 is the electrical permittivity of free space, $\tau_e(t,r,z)$ is the free electron relaxation time, and ω is the laser frequency. The complex dielectric function can be split into the real and imaginary components as follows:

$$\boldsymbol{\epsilon}(t,r,z) = \epsilon_1(t,r,z) + i\epsilon_2(t,r,z) = \left[1 - \frac{\omega_p^2(n_e)\tau_e^2(t,r,z)}{1+\omega^2\tau_e^2(t,r,z)}\right] + i\left\{\frac{\omega_p^2(n_e)\tau_e(t,r,z)}{\omega[1+\omega^2\tau_e^2(t,r,z)]}\right\}, \quad (4)$$

where $\boldsymbol{\epsilon}$ is the complex dielectric function, ϵ_1 is the real component of dielectric function, and ϵ_2 is the imaginary component of dielectric function.

The relationship between the complex refractive index **f** and the complex dielectric function is given by

$$(\mathbf{c}/\mathbf{v}) = \mathbf{f} = (f_1 + if_2) = \sqrt{\boldsymbol{\epsilon}} = \sqrt{\epsilon_1 + i\epsilon_2}, \quad (5)$$

where **c** is the velocity of light in vacuum, **v** is the velocity of light in the material, f_1 is the normal refractive index, and f_2 is the extinction coefficient. Thus, the f_1 and f_2 functions are

$$f_1(t,r,z) = \sqrt{\frac{\epsilon_1(t,r,z) + \sqrt{\epsilon_1^2(t,r,z) + \epsilon_2^2(t,r,z)}}{2}},$$

$$f_2(t,r,z) = \sqrt{\frac{-\epsilon_1(t,r,z) + \sqrt{\epsilon_1^2(t,r,z) + \epsilon_2^2(t,r,z)}}{2}}. \quad (6)$$

The reflectivity of the ionized material is determined by the following Fresnel expression at the surface

$$R(t,r) = \frac{[f_1(t,r,0)-1]^2 + f_2^2(t,r,0)}{[f_1(t,r,0)+1]^2 + f_2^2(t,r,0)}. \quad (7)$$

The absorption coefficient of laser intensity by the plasma via the free electron heating is calculated by

$$\alpha_h(t,r,z) = \frac{2\omega f_2(t,r,z)}{c}. \quad (8)$$

Note that Eq. (8) represents only a part of the laser energy that is absorbed via free electron heating, and there is another part of absorption that is via ionization. The total absorption coefficient α accounting for both the free electron heating absorption and the absorption through impact ionization and photoionization is derived as

$$\alpha(t,r,z) = \{a_i n_e(t,r,z) + \delta_N[I(t,r,z)]^{N-1}\} \times [\langle\varepsilon(t,r,z)\rangle + U_I], \quad (9)$$

where $\langle\varepsilon(t,r,z)\rangle$ is the average kinetic energy of free electrons and U_I is the band gap of materials. For fused silica, U_I=9 eV.

D. Free electron heating: Electron relaxation time

The free electron relaxation time in Eq. (3) is calculated by the following quantum estimation derived from the Boltzmann transportation equation[21]

$$\tau_e(t,r,z) = \frac{3\sqrt{m_e}[k_B T_e(t,r,z)]^{3/2}}{2\sqrt{2}\pi(Z^*)^2 n_e(t,r,z)e^4 \ln\Lambda \times\{1+\exp[-\mu(n_e,T_e)/k_B T_e(t,r,z)]\}F_{1/2}}, \quad (10)$$

where Z^* is the ionization state, k_B is the Boltzmann constant, T_e is the electron temperature, $F_{1/2}$ is the Fermi–Dirac integrals, μ is the chemical potential, and $\ln\Lambda$ is the Coulomb logarithm determined by[22]

$$\ln\Lambda = \frac{1}{2}\ln\left[1 + \left(\frac{b_{\max}}{b_{\min}}\right)^2\right], \quad (11)$$

where the maximum ($b_{\max}$) and minimum ($b_{\min}$) collision parameters are given by

$$b_{\max} = \frac{(k_B T_e/m_e)^{1/2}}{\max(\omega,\omega_p)}, b_{\min} = \max\left(\frac{Ze^2}{k_B T_e}, \frac{h}{2\pi(m_e k_B T_e)^{1/2}}\right), \quad (12)$$

where ω is the laser frequency, ω_p is the plasma frequency, Z is the charge state of ions, and h is the Planck constant.

However, at the very beginning of laser ablation, the electron kinetic energy is relatively low, contributions to the free electron relaxation time from electron-phonon collisions could be important. Hence, in this study when the electron kinetic energy is lower than or comparable to the Fermi energy, both the contributions of electron-phonon and electron-ion collisions are considered, and the free electron relaxation time is determined by[22]

$$\tau_e = \frac{1}{\nu_e} = \frac{1}{\nu_{ei}} + \frac{1}{\nu_{ep}}, \quad (13)$$

where ν_e is the electron collision frequency, ν_{ei} is the electron-ion collision frequency, and ν_{ep} is the electron-phonon collision frequency determined by

$$\frac{1}{\nu_{ep}} = \left(\frac{M}{m_e}\right)^{1/2}\frac{\hbar}{U_{IP}}\frac{T_D}{T_l}\left(\frac{n_e(t,r,z)}{n_{cr}}\right)^{1/3}, \quad (14)$$

where M is the atomic mass unit, $\hbar = h/2\pi$ is the reduced Planck constant (h is the Planck constant), U_{IP} is the ionization potential that is 13.6 eV for fused silica,[20] T_D is the Debye temperature (290 K for fused silica), and T_l is the lattice temperature in K.

For free electrons modeled as "particle in a box," the chemical potential can be calculated by[23]

$$\mu(n_e,T_e) = \varepsilon_F(n_e) \times \left[1 - \frac{\pi^2}{12}\left(\frac{k_B T_e(t,r,z)}{\varepsilon_F(n_e)}\right)^2 + \frac{\pi^2}{80}\left(\frac{k_B T_e(t,r,z)}{\varepsilon_F(n_e)}\right)^4\right], \quad (15)$$

where the higher order terms are neglected and ε_F is the Fermi energy that is determined by

$$\varepsilon_F(n_e) = \left[\frac{(hc)^2}{8m_e c^2}\right] \times \left(\frac{3}{\pi}\right)^{2/3} \times [n_e(t,r,z)]^{2/3}, \quad (16)$$

where c is the scalar speed of light in vacuum.

In the first type of assumptions, it is assumed that a small volume of material is ablated if its free electron density is equal to or above the critical electron density. For femtosecond lasers, the critical density n_{cr} is selected as the free electron density at which the plasma oscillation frequency is equal to the laser frequency. Thus, according to Eq. (3),

$$n_{\mathrm{cr}} = \frac{4\pi^2 c^2 m_e \epsilon_0}{\lambda^2 e^2}, \tag{17}$$

where λ is the wavelength of the laser.

E. Electron-phonon interaction: Free electron heating

Because the dielectric material is first transformed into absorbing plasma with metallic properties by strong ionization before phase change occurs, the improved two-temperature model[3] can be applied to describe the electron-phonon interaction in the impact area

$$C_e(T_e)\frac{\partial T_e(t,r,z)}{\partial t} = \nabla(k_e(T_e)\nabla T_e) - G(T_e - T_l) + S(t,r,z) - H_e(t,r,z), \tag{18}$$

$$C_l(T_l)\frac{\partial T_l(t,r,z)}{\partial t} = \nabla(k_l \nabla T_l) + G(T_e - T_l) - H_l(t,r,z), \tag{19}$$

where S represents the laser source term, C_e is the specific heat of free electrons, C_l is the lattice heat capacity, k_e is the electron conductivity, k_l is the lattice conductivity, H_e is the energy loss due to electron escape, G is the electron-lattice coupling factor, and H_l is the energy loss due to the lattice removal which includes the latent heat and sensible heat

$$H_l = \int_{T_m}^{T_l} C_l(T)dT + H_{\mathrm{latent}}. \tag{20}$$

Glasses such as fused silica do not have the latent heat of phase change.[24,25] Note that this assumption does not apply for some other materials such as metals in which the latent heats of melting and vaporization are nonzero.

The free electron heat conductivity is expressed by the following Drude theory of metals[23]

$$k_e(T_e) = \frac{1}{3}v_e^2(T_e)\tau_e(T_e)C_e(T_e), \tag{21}$$

where v_e^2 is the mean square of electron speed. In this study, v_e^2 and C_e are determined directly by the Fermi distribution. Actually, phonon heat capacity is also temperature-dependent, which can be calculated by the Debye model.[3]

In Eq. (19), the electron-lattice coupling factor is estimated by[26]

$$G = \frac{\pi^2 m_e n_e(t,r,z)c_s^2}{6\tau(T_e)T_e(t,r,z)}, \tag{22}$$

where c_s is the speed of sound in bulk material calculated by

$$c_s = \sqrt{\frac{B}{\rho_m}}, \tag{23}$$

where B is the bulk modulus and ρ_m is the density.

In Eq. (18), the energy source through electron heating, $S(t,r,z)$, is determined by

$$S(t,r,z) = \frac{\alpha_h(t,r,z)I(t,r,z)}{n_e(t,r,z)}. \tag{24}$$

The energy loss H_e is given as

$$H_e(t,r,z) = c_h \int_{\varepsilon_F+\varepsilon_W}^{\infty} \frac{1}{e^{\beta(T_e)[\varepsilon-\mu(n_e,T_e)]}+1}\rho(\varepsilon)\varepsilon d\varepsilon, \tag{25}$$

where ε_W is the work function, $\rho(\varepsilon)$ is the density of states, and c_h is a statistic energy loss coefficient on which we are still investigating by using *ab initio* molecular dynamics and statistic methods.

In Eq. (25), $\beta(T_e)=1/k_B T_e(t,r,z)$ and $\rho(\varepsilon)$ is the density of states given by

$$\rho(\varepsilon) = \frac{8\sqrt{2}\pi m_e^{3/2}}{h^3}\sqrt{\varepsilon}. \tag{26}$$

In Eq. (18), C_e is calculated by

$$C_e(T_e) = \left(\frac{\partial\langle\varepsilon\rangle}{\partial T_e}\right)_V n_e(t,r,z). \tag{27}$$

The average kinetic energy $\langle\varepsilon\rangle$ is determined by the Fermi–Dirac distribution

$$\langle\varepsilon\rangle = \frac{\sum_k \langle n_k\rangle\varepsilon_k}{N_e} = \frac{\int_0^{\infty} \frac{1}{e^{\beta(T_e)[\varepsilon-\mu(n_e,T_e)]}+1}\rho(\varepsilon)\varepsilon d\varepsilon}{\int_0^{\infty} \frac{1}{e^{\beta(T_e)[\varepsilon-\mu(n_e,T_e)]}+1}\rho(\varepsilon)d\varepsilon}, \tag{28}$$

where $\langle n_k\rangle$ is the average number of electrons in energy state and N_e is the total number of free electrons.

However, there still remain two unresolved challenges regarding G and H_e: neither Eq. (22) nor (25) is generally applicable for the dense plasma with a changing electron density and temperature, on which we are still working.

III. RESULTS AND DISCUSSION

A. Fixed processing window

In the limit of negligible recast, by using free electron density based assumptions, ablation depth is considered to be the maximum depth at which the maximum free electron density is equal to the critical density in a given processing window. By using the lattice temperature-based assumptions, ablation depth is considered to be the maximum depth at which the lattice temperature is equal to the melting point.

For the case of fixed processing parameters, a λ =780 nm pulse with t_p=50 fs and r_0=50 μm Gaussian beam profile is used for the ablation of fused silica, and the calculated results are compared with experimental measurements to validate the models. The experimental ablation threshold fluence is about 3.3 J/cm^2, and the corresponding experimental ablation depth at 5 J/cm^2 is about 200 nm.[2] The plasma model based on free electron density gives the results of 3.15 J/cm^2 and 195 nm, respectively, for the threshold fluence and ablation depth, while the plasma model plus two-temperature equation based on lattice temperature gives the results of 3.1 J/cm^2 and 200 nm, respectively. The predictions based on the two types of assumptions are in agreement with each other and experimental data.[2]

The ablation crater shapes predicted by using the two types of assumptions at the laser fluence of 5 J/cm^2 by a

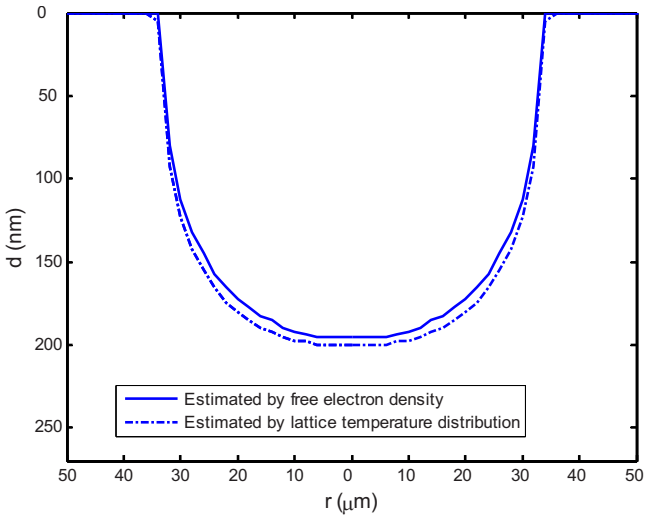

FIG. 1. (Color online) The ablation crater shapes predicted by the plasma model and plasma model plus two-temperature equation.

780 nm and 50 fs laser pulse are shown in Fig. 1. The prediction of the plasma model is similar to that of the plasma model plus the two-temperature equation in terms of both ablation shape and size. Both predicted ablation shapes at 5 J/cm^2 are rather flat at the bottom as compared to the Gaussian profile. At higher fluences, the flat-bottom crater is even more obvious.[16] Such type of flat-bottom crater shapes has been observed in previous experiments on ultrashort laser ablation of other materials.[27–29] Generally, in the femtosecond laser ablation of wide band gap materials, craters with a flat-bottom should be formed, although the degree of flatness depends on the ablation fluence and duration, which is also confirmed by the model based on the temperature assumptions.

The flat-bottom crater is caused by the significant changes in the reflectivity and absorption coefficient of the generated plasma, as shown in Fig. 2, which shapes the transmitted laser intensity shown in Fig. 3. It is clearly seen that after the critical free electron density is reached (at 27 fs), the laser intensity distribution in the material is strongly reshaped. The differences between the original laser intensity

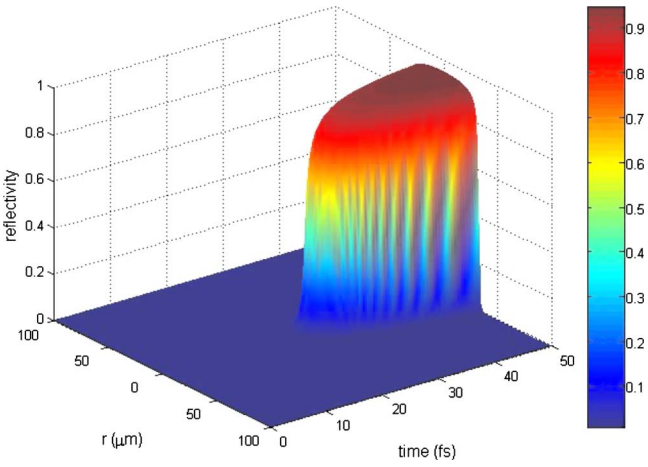

FIG. 2. (Color online) The temporal and spatial dependent reflectivity of generated dense plasma in fused silica.

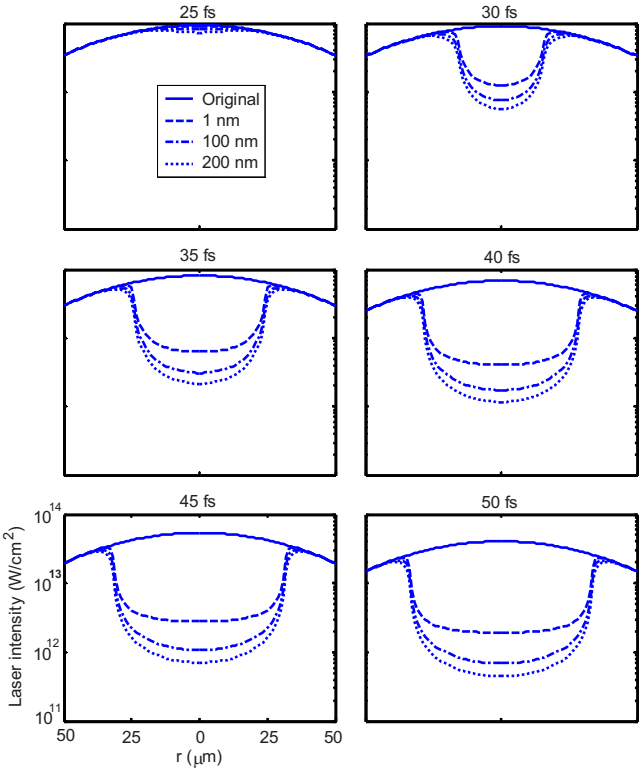

FIG. 3. (Color online) The laser intensity distribution as a function of radius at different depths and times: $t_p=50$ fs, $F=5$ J/cm^2.

profile and the profile at 1 nm are mainly caused by reflection. As shown in Fig. 3, the laser intensity at 1 nm remains nearly constant after 40 fs. On the other hand, the differences of laser intensity at 1 nm and that at 100 nm are due to the absorption of the laser energy by the plasma between these two depths.

In this subsection, the assumption that "the ablation crater shape corresponds to the region at which the free electron density is greater than or equal to the critical density" is validated by the comparison study. The plasma model plus two-temperature model also theoretically confirms the flat-bottom phenomenon.[16] However, the underlying mechanisms must be interpreted by free electron density distribution instead of lattice temperature, which demonstrates the advantage of the plasma model.

B. The effects of fluence

Fluence is one of the most important factors for ablation depth and crater shape. As shown in Fig. 4, the ablation depths by the 780 nm, 220 fs laser as a function of the fluence well explain the crater shapes plotted in Fig. 1. The ablation depths predicted by using the two types of assumptions are visually the same. From about 7.0 to 12 J/cm^2, the ablation depth increases relatively slowly. The existence of a nearly constant ablation depth after a steep increase was experimentally observed before.[30–32]

Based on Beer's law with constant optical properties, the following equation has been used to predict the ablation depth as a function of fluence[33]

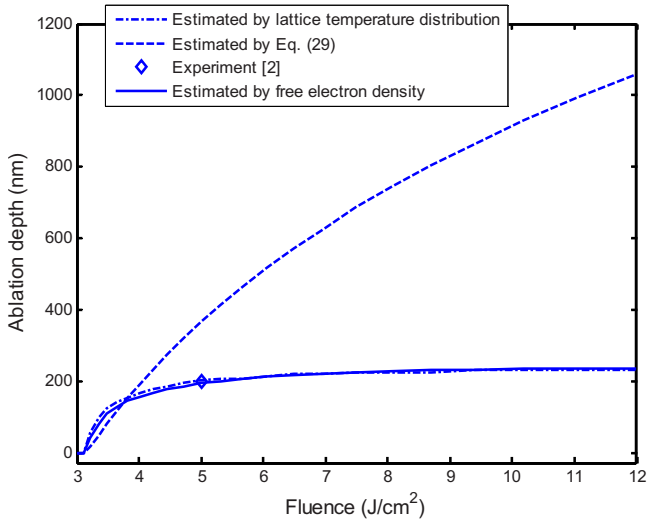

FIG. 4. (Color online) Ablation depths in fused silica at different fluences by a 780 nm, 220 fs, and 5 J/cm^2 pulse.

$$d = \left(\frac{1}{\alpha}\right)\ln\frac{F}{F_{\text{th}}}, \tag{29}$$

where F_{th} is the threshold fluence. As the absorption coefficient of the material varies significantly as a function of time, space, and laser intensity during the femtosecond laser irradiation, the selection of a "correct" constant absorption coefficient is very challenging if not impossible. If a mean absorption coefficient over the space and the fluence is used, Eq. (29) predicts the ablation depth as shown in Fig. 4, which is not consistent with the experimental result.

The constant ablation depth zone occurs because the overall reflectivity and absorption coefficient significantly increase with the increase in fluence as shown in Fig. 5. For $r=0$ and $t=25$ fs, the absorption coefficients in the surface layer (numerically 1 nm) at 5, 6, and 10 J/cm^2 are 1.26×10^4, 7×10^4, and 2.4×10^5 cm^{-1}, respectively. The formation of a thin skin depth at higher fluences becomes more obvious, which strongly affects the ablation depth and crater shape.[34] Also, the overall reflectivity integrated in the whole

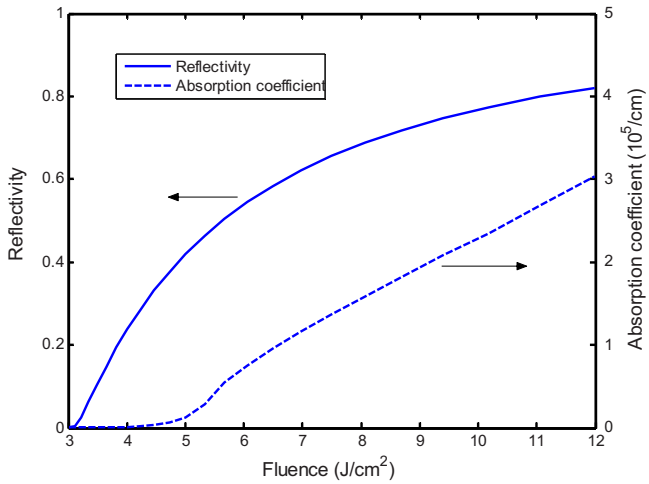

FIG. 5. (Color online) Integrated reflectivity and absorption coefficient in fused silica surface layer (numerically 1 nm) at $t=25$ fs.

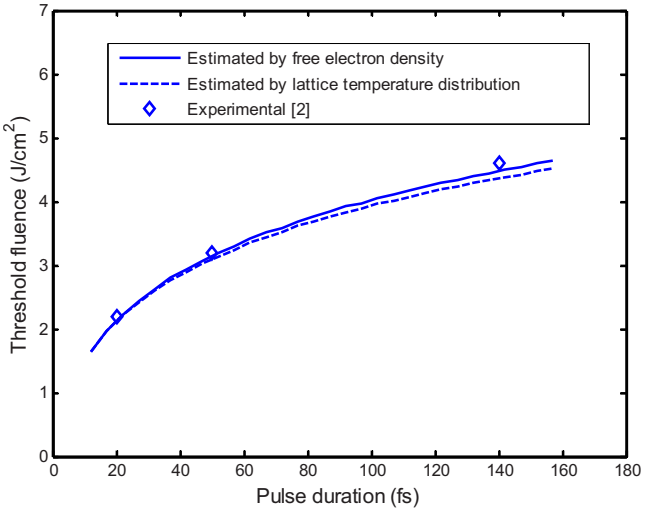

FIG. 6. (Color online) Threshold fluence as a function of pulse duration for fused silica.

pulse duration increased with fluences: 5, 6, and 10 J/cm^2 are 0.42, 0.55, and 0.77, respectively. Note the constant ablation depth exists only in a limited fluence range, and the ablation depth may significantly increase if the fluence continues to increase.[30,31]

In this subsection, the phenomenon of the constant ablation depth zone is confirmed by the plasma model plus the two-temperature equation. However, the plasma optical properties determined by the electron dynamics instead of lattice temperature are still the key to the fundamental understanding of this phenomenon.

C. The effects of pulse duration

Another important parameter for laser ablation is the pulse duration. Figures 6 and 7 show the threshold fluence and ablation depth as the functions of pulse duration, respectively. It is seen that the predictions by the plasma model and the plasma model plus the two-temperature equation are both in agreement with the experimental results.[2] The trends predicted by both models are the same. The threshold fluence

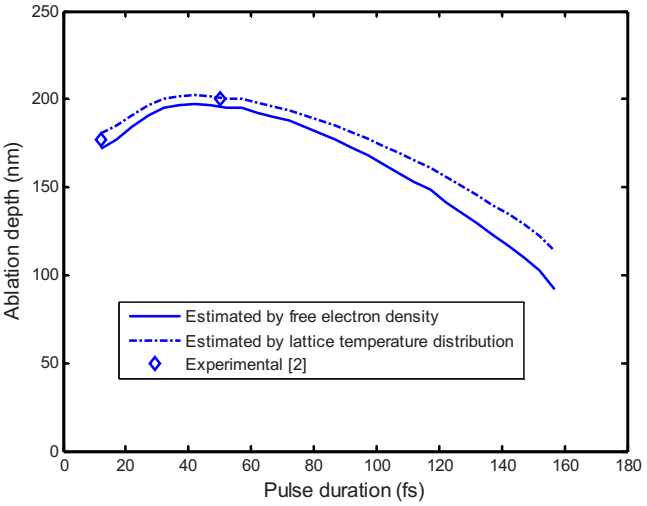

FIG. 7. (Color online) Threshold fluence and ablation depth as a function of pulse duration, $F=5$ J/cm^2 for ablation depth calculations.

increases as pulse duration increases, as expected. However, the ablation depth by a 780 nm laser at 5 J/cm^2 is not a monotonous function of the pulse duration, as shown in Fig. 7. When the pulse duration is very short and the laser fluence is "strong" with respect to the corresponding threshold fluence, the ablation depth increases as the pulse duration increases. Figure 7 shows that the ablation depth increases with the increase in pulse duration in the range of 10–50 fs.. However, when the pulse duration increases to some point, the fluence becomes "weak" with respect to the corresponding threshold fluence, thereafter the ablation depth decreases as the pulse duration increases. Figure 7 shows that ablation depth decreases with the increase in pulse duration in the range of 50–160 fs..

The comparison studies on threshold fluence and ablation depth as functions of pulse duration validates the following two assumptions, (1) threshold fluence can be considered as the minimal fluence that just creates the critical density and (2) ablation depth can be considered to be the maximum depth at which the maximum free electron density is equal to the critical density in a given processing window. In the limit of negligible recast and phase change dominated by nonthermal ablation, the plasma model is applicable. Also, the important trends and phenomena discussed earlier can be interpreted by free electron distribution instead of lattice temperature distribution. Further, the plasma model is less complex than the combined model. Finally, at this time, the energy loss due to electron escape and the electron-lattice coupling factor cannot be precisely determined in a general form for the dense plasma, which limits the application of the two-temperature equation in femtosecond ablation of dielectrics.

On the other hand, if recast occurs and multiple phase change mechanisms coexist, the Coulomb explosion and electrostatic ablation, the lattice change must be taken into consideration. In general cases, it is necessary to include the plasma model, two-temperature model (or Boltzmann transport equation), molecular dynamics, and so on in a multiscale model to reveal the ablation process, on which our current efforts are being focused.

IV. CONCLUSIONS

By combining the plasma model with the improved two-temperature model, this study validates the assumptions based on free electron density for material removals during femtosecond laser ablation of dielectrics through nonthermal processes. The threshold fluences, ablation depths, and shapes of fused silica, predicted by using (1) the plasma model only and (2) the plasma model plus the two-temperature equation, are in agreement with each other and the published experimental data. The trends and phenomena such as flat-bottom crater shape and constant ablation depth zone predicted by both models are essentially the same. The widely used assumptions for threshold fluence, ablation depth, and shape in the plasma model based on free electron density are validated by the experiments and the counter assumptions in the combined model based on lattice temperature. In the limit of negligible recast and phase change dominated by nonthermal ablation, the plasma model is applicable with advantages of relative simplicity and acceptable precision.

However, further efforts are required to precisely determine the energy loss due to electron escape and the electron-lattice coupling factor in the two-temperature equation for generated dense plasma with the temporal and spatial dependent free electron density. Also, a scientific understanding of the general cases of femtosecond ablation requires a multiscale model, which may include the plasma model, two-temperature model (or Boltzmann transport equation), and other nanoscale methodologies such as (*ab initio* and/or classical) molecular dynamics.

ACKNOWLEDGMENTS

This work was supported by the Air Force Research Laboratory USA under Contract No. FA8650-04-C-5704, the National Science Foundation USA under Grant No. 0423233, the National Natural Science Foundation China under Grant No. 50705009, and the 111 Project China under Grant No. B08043.

[1] L. Jiang and H. L. Tsai, Appl. Phys. Lett. **87**, 151104 (2005).
[2] M. Lenzner, J. Krüger, S. Sartania, Z. Cheng, C. Spielmann, G. Mourou, W. Kautek, and F. Krausz, Phys. Rev. Lett. **80**, 4076 (1998).
[3] L. Jiang and H. L. Tsai, ASME J. Heat Transfer **127**, 1167 (2005).
[4] B. Rethfeld, A. Kaiser, M. Vicanek, and G. Simon, Phys. Rev. B **65**, 214303 (2002).
[5] T. Q. Qiu and C. L. Tien, Int. J. Heat Mass Transfer **37**, 2789 (1994).
[6] F. Ladieu, P. Martin, and S. Guizard, Appl. Phys. Lett. **81**, 957 (2002).
[7] H. E. Elsayed-Ali, T. B. Norris, M. A. Pessot, and G. A. Mourou, Phys. Rev. Lett. **58**, 1212 (1987).
[8] T. Hertel, E. Knoesel, M. Wolf, and G. Ertl, Phys. Rev. Lett. **76**, 535 (1996).
[9] S. D. Brorson, A. Kazeroonian, J. S. Moodera, D. W. Face, T. K. Cheng, E. P. Ippen, M. S. Dresselhaus, and G. Dresselhaus, Phys. Rev. Lett. **64**, 2172 (1990).
[10] L. Jiang and H. L. Tsai, Proceedings of the NSF Workshop on Research Needs in Thermal Aspects of Material Removal, Stillwater, OK, 2003 (unpublished), p. 163.
[11] R. Stoian, D. Ashkenasi, A. Rosenfeld, and E. E. B. Campbell, Phys. Rev. B **62**, 13167 (2000).
[12] B. C. Stuart, M. D. Feit, S. Herman, A. M. Rubenchik, B. W. Shore, and M. D. Perry, Phys. Rev. B **53**, 1749 (1996).
[13] B. C. Stuart, M. D. Feit, A. M. Rubenchik, B. W. Shore, and M. D. Perry, Phys. Rev. Lett. **74**, 2248 (1995).
[14] M. D. Perry, B. C. Stuart, P. S. Banks, M. D. Feit, V. Yanovsky, and A. M. Rubenchik, J. Appl. Phys. **85**, 6803 (1999).
[15] L. Jiang and H. L. Tsai, J. Phys. D **37**, 1492 (2004).
[16] L. Jiang and H. L. Tsai, Int. J. Heat Mass Transfer **48**, 487 (2005).
[17] E. G. Gamaly, A. V. Rode, B. Luther-Davies, and V. T. Tikhonchuk, Phys. Plasmas **9**, 949 (2002).
[18] X. Xu, G. Chen, and K. H. Song, Int. J. Heat Mass Transfer **42**, 1371 (1999).
[19] M. Li, S. Menon, J. P. Nibarger, and G. N. Gibson, Phys. Rev. Lett. **82**, 2394 (1999).
[20] M. Fox, *Optical Properties of Solids* (Oxford University Press, Oxford, 2001).
[21] Y. T. Lee and R. M. More, Phys. Fluids **27**, 1273 (1984).
[22] K. Eidmann, J. Meyer-ter-Vehn, T. Schlegel, and S. Hüller, Phys. Rev. E **62**, 1202 (2000).
[23] N. W. Ashcroft and N. D. Mermin, *Solid State Physics* (Holt, Rinehart, and Winston, New York, 1976).
[24] R. H. Doremus, *Glass Science* (Wiley, New York, 1994).
[25] A. Rousse, C. Rischel, S. Fourmaux, I. Uschmann, S. Sebban, G. Grillon, P. Balcou, E. Förster, J. P. Geindre, P. Audebert, J. C. Gauthier, and D. Hulin, Nature (London) **410**, 65 (2001).
[26] T. Q. Qiu and C. L. Tien, Int. J. Heat Mass Transfer **35**, 719 (1992).

[27]G. Dumitru, V. Romano, H. P. Weber, M. Sentis, and W. Marine, Appl. Phys. A: Mater. Sci. Process. **74**, 729 (2002).
[28]Z. Wu, H. Jiang, Z. Zhang, Q. Sun, H. Yang, and Q. Gong, Opt. Express **10**, 1244 (2002).
[29]J. Bonse, M. Munz, and H. Sturm, IEEE Trans. Nanotechnol. **3**, 358 (2004).
[30]S. Nakamura, M. Hoshino, and Y. Ito, Proceedings of the ICALEO, Jacksonville, FL, 2001 (unpublished).
[31]M. Lapczyna, K. P. Chen, P. R. Herman, H. W. Tan, and R. S. Marjoribanks, Appl. Phys. A: Mater. Sci. Process. **69**, S883 (1999).
[32]P. R. Herman, A. Oettl, K. P. Chen, and R. S. Marjoribanks, Proc. SPIE **3616**, 148 (1999).
[33]J. Krüger and W. Kautek, Laser Phys. **9**, 30 (1999).
[34]L. Jiang and H. L. Tsai, J. Appl. Phys. **100**, 023116 (2006).